
Article:
Fragiadaki, M., Lannoy, M., Themanns, M. et al. (5 more authors) (2017) STAT5 drives abnormal proliferation in autosomal dominant polycystic kidney disease. Kidney International. ISSN 0085-2538

https://doi.org/10.1016/j.kint.2016.10.039

STAT5 drives abnormal proliferation in autosomal dominant polycystic kidney disease.

Maria Fragiadaki[1§], Morgane Lannoy[1], Madeleine Themanns[2], Barbara Maurer[2], Wouter N Leonhard[3], Dorien JM Peters[3], Richard Moriggl[2] Albert CM Ong[1]

[1] Academic Nephrology Unit, Department of Infection, Immunity and Cardiovascular Disease, The Medical School, University of Sheffield, Sheffield, UK, S10 2RX
[2] Ludwig Boltzmann Institute for Cancer Research, University of Veterinary Medicine, Vienna, Medical University Vienna, Austria, A-1090
[3] Department of Human Genetics, Leiden University Medical Center (LUMC), Leiden, Netherlands, 2300RC

Running Head: STAT5 in polycystic kidney disease

[§] Correspondence: Maria Fragiadaki, Academic Unit of Nephrology, Department of Infection, Immunity and Cardiovascular Disease, University of Sheffield.
Email: m.fragiadaki@sheffield.ac.uk
Telephone: +44 011427 12842

Abstract word count: (limit 1500 characters including spaces)
Text word count: (limit 4000)

Autosomal dominant polycystic kidney disease (ADPKD) leads to renal failure. The hallmark of ADPKD is increased epithelial proliferation, which has been proposed to be due to atypical signalling including abnormal JAK-STAT activity. However, the relative contribution of JAK-STAT family members in promoting proliferation in ADPKD is unknown. Here we present an siRNA JAK-STAT focused screen revealing a previously unknown proliferative role for multiple JAK-STAT components (including STAT1, STAT2, STAT4, STAT5a, STAT5b). Amongst these we selected to study the GH-GHR-STAT5-axis because of its known role as a regulator of growth in non-renal tissues. We show that STAT5 loss of function, facilitated by pharmacological inhibition or siRNAs, significantly reduced proliferation with an associated reduction in cyst growth *in vitro*. To study whether STAT5 is abnormally activated *in vivo*, we analyzed its expression using two independent mouse models of ADPKD. STAT5 was nuclear, thus activated, in renal epithelial cyst lining cells in both. To test whether forced activation of STAT5 can modulate proliferation of renal cells *in vivo*, irrespective of *Pkd1* status, we overexpressed growth hormone (GH). GH mice showed increased STAT5 activity in renal epithelial cells, correlating with *de-novo* expression of cyclin D1, a STAT5 target gene. Chromatin immunoprecipitations, revealed that STAT5 transcriptionally activated cyclin D1 in GH-stimulated renal epithelial but not control cells, thus providing a mechanism into how STAT5 enhances proliferation. Finally, we provide evidence of elevated GH in $Pkd1^{nl/nl}$ mice. Collectively, our data identify the GH-STAT5 signalling axis as a novel therapeutic target in ADPKD.

INTRODUCTION

Autosomal dominant polycystic kidney disease (ADPKD), a major cause of renal replacement therapy [1], frequently arises due to mutations in polycystic kidney disease 1 (PKD1) [2]. The hallmark of ADPKD is fluid-filled cysts originating from tubular epithelial cells [3, 4]. They exhibit a hyper-proliferative and pro-apoptotic phenotype [5], eventually leading to end-stage renal disease. Tolvaptan, a v2-specific vasopressin receptor antagonist, is the first drug approved for the treatment of ADPKD, however additional therapeutic targets are needed because tolvaptan is not curative and side effects preclude treatment in some patients [6].

The JAnus Kinase and Signal Transducers and Activators of Transcriptions (JAK-STAT) is an evolutionarily-conserved pathway controlling G1-S cell cycle progression [7]. It consists of 7 transcription factors (STAT1-5a, STAT5b and STAT6) and 4 tyrosine kinases (JAK1-3 and Tyk2). JAK-STAT is activated by several cytokines, including GH, IFNγ and OSM [8]. Previous work linked abnormal *Pkd1* expression with altered JAK-STAT activity. Specifically, STAT1 interaction with the c-terminus of PKD1 leads to a pro-quiescent signal, thus reducing proliferation of renal epithelial cells [9]. Antithetically, STAT6 promotes proliferation via binding to a cleaved c-terminal fragment of PKD1 [10]; moreover global knockout of STAT6 suppresses cyst growth [11]. Accordingly, the c-terminus of PKD1 also activates STAT3 in ADPKD [12]. Finally, inhibition of STAT3 has been associated with reduced cyst growth in ADPKD murine models [13, 14]. However, the relative contribution of core components of the JAK-STAT pathway and activating cytokines in driving ADPKD has not been studied. To address this, we performed an unbiased screen of JAK-STAT pathway to determine their contribution to epithelial proliferation in ADPKD. Our study reveals an unexpected involvement of multiple JAK-STAT components. We focus subsequent studies on GH-activated STAT5 signalling, since this pathway has a validated function in control of tissue growth but has not been studied in the context of ADPKD previously.

RESULTS

GH-GHR-STAT5 axis identified as a putative pro-proliferative arm in ADPKD.

To discover novel components of the JAK-STAT pathway that control pathogenic proliferation of epithelial cells in ADPKD, we performed a JAK-STAT focused RNAi screen of 29 genes using human renal epithelial cystic cells from a patient with ADPKD (OX161; [15]). The siRNAs targeted core components of the JAK-STAT pathway, cytokines and their cognate receptors. Following siRNA treatment, the proliferative capacity of OX161-cells, was measured by proliferating cell nuclear antigen (PCNA) staining and analyzed by the one-way ANOVA test. To validate the screen, we demonstrated that PCNA and cyclin D1 siRNA caused a significant reduction in proliferation when compared to non-target RNAi treated cells (Figure 1A). We also performed Western blotting to confirm that siRNA resulted in reduction of STAT protein levels (SI1). Interestingly, silencing of numerous JAK-STAT related genes significantly reduced proliferation of OX161 cystic cells (Figure 1B-1E). To investigate the interactions of identified genes and place them in functionally-related pathways we performed DAVID functional annotation, which identified a cluster of 6 genes that regulate growth, namely GH, GH receptor (GHR), STAT5a, STAT5b, interferon gamma (IFNγ) and oncostatin M (OSM). Because the GH-GHR-STAT5 axis controls proliferation and body-growth and its involvement in ADPKD is currently unknown, we decided to focus the rest of our study on this.

Figure 1: The JAK-STAT siRNA screen

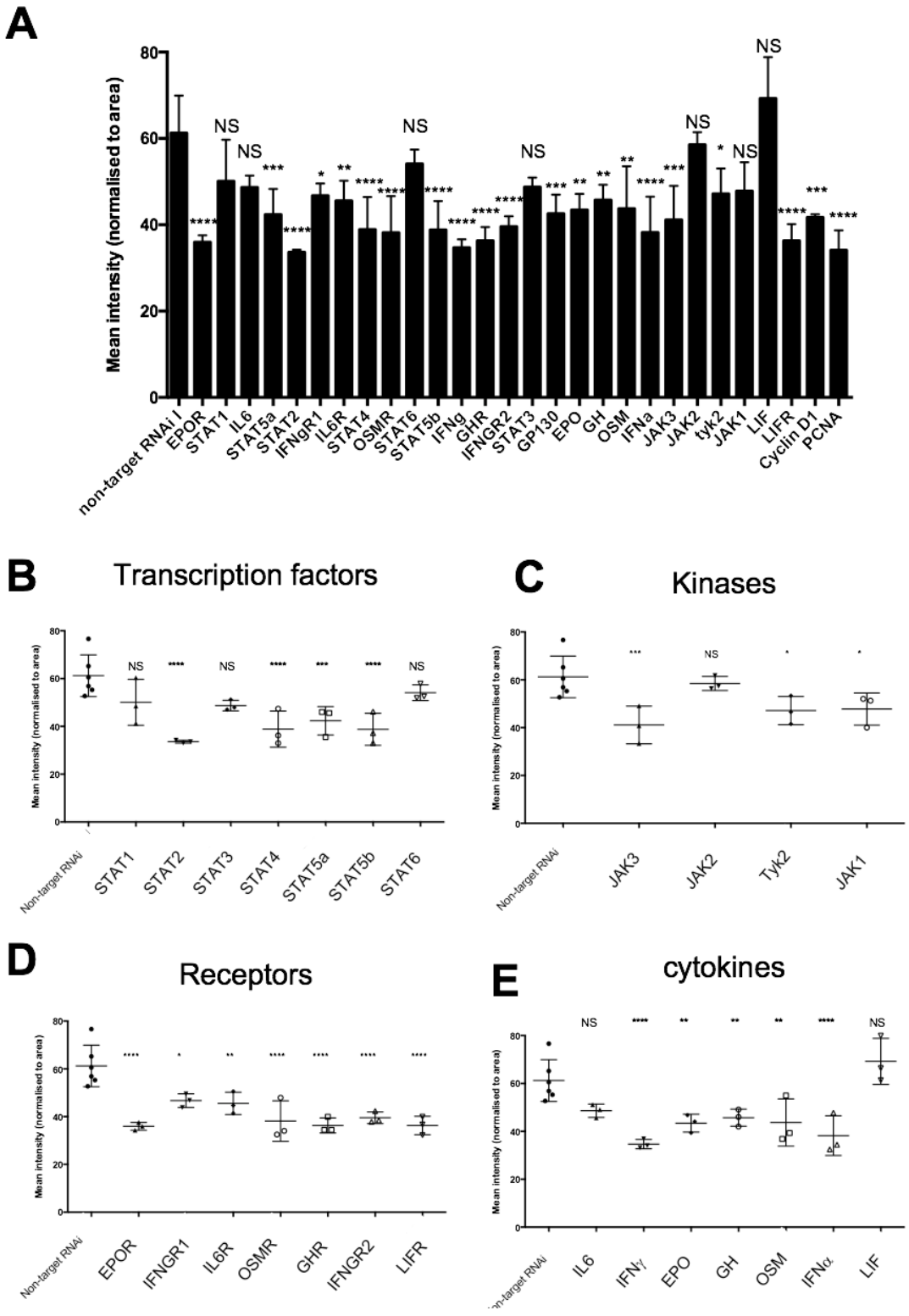

STAT5 regulates proliferation but not apoptosis in ADPKD.
To validate the effects of STAT5 in controlling proliferation of ADPKD-derived cells we employed an additional independent siRNA and a selective STAT5 small

molecule inhibitor (VWR-573108 [16]). We confirmed that VWR-573108 reduced phosphorylation of STAT5 without affecting STAT1/3 phosphorylation, demonstrating selectivity (SI Fig 1B). Using both OX161 and SKI-001 we found that siRNA silencing or VWR-57108 inhibitor significantly reduced proliferation (Figure 2A and 2B). We then performed flow cytometry in cells with STAT5 siRNA or non-target RNAi controls for the mitosis markers, histone H3 (ser10). Flow cytometry showed that silencing of STAT5 led a significant reduction in the marker of mitosis when compared to control (Fig 2C). Collectively these data suggest that STAT5 supports proliferation in ADPKD-derived cells. To study whether STAT5 loss-of-function affects proliferation in Pkd1 wild-type cells we used mouse Pkd1 wild-type epithelial cells (F1 $Pkd1^{WT/WT}$) and compared their response to Pkd1-null (F1- $Pkd1^{-/-}$) cells. We found that STAT5 silencing led to a significant reduction in proliferation in Pkd1 null but not wild-type cells (SI Fig 1C and C'). Finally, measurement of cleaved caspase-3 demonstrated that inhibition of STAT5 did not significantly alter the rate of apoptosis (Figures 2D and 2D'). Collectively, these data indicate that inhibition of STAT5 prevents proliferation without affecting apoptosis in Pkd1 mutant cells.

Figure 2: STAT5 is a positive regulator of proliferation in cystic epithelial cells.

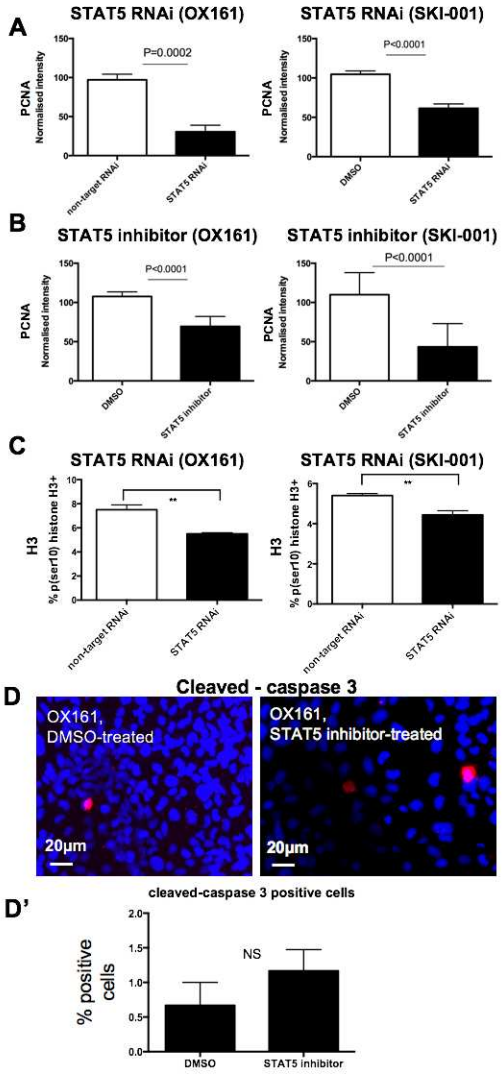

Nuclear STAT5 expression is increased in two independent models of ADPKD (*Pkd1* modulation)

To study the expression and activation of STAT5 in cells with and without deletion of the *Pkd1* gene *in vivo*, we used the previously published hypomorphic *Pkd1*$^{nl/nl}$ mutant mouse, where *Pkd1* expression is reduced to approximately 15% [17]. Heterozygote mice were bred to obtain homozygote offspring and wild-type littermate controls, which survived up to the age of 10 weeks. *Pkd1*$^{nl/nl}$ mice developed progressive polycystic kidney disease, whereas kidneys of wild-type littermates appeared normal (Figure 3A). We used kidney sections from such mice to examine expression of STAT5 at 4 and 8 and 10 weeks of age. Immunohistochemistry revealed that STAT5 was often expressed in cyst-lining epithelial cells in *Pkd1*$^{nl/nl}$ at all time points studied and its expression was strongly nuclear (Figure 3). There was a significantly higher percentage of nuclear STAT5 in *Pkd1*$^{nl/nl}$ mice compared to age-matched wild-type littermate controls at all time points (Figure 3B). We then examined the relative STAT5 expression during disease progression in *Pkd1*$^{nl/nl}$ mice and found that STAT5 expression was the highest at 4 weeks of age and its expression declined by 10 weeks in both Pkd1 wild-type and *Pkd1*$^{nl/nl}$ (Figure 3). Coincidentally, the kidneys of 10 week-old *Pkd1*$^{nl/nl}$ mice exhibited diffuse fibrosis consistent with previous reports [17], suggesting that mice at this age exhibited late-stage disease. In summary, there is a higher percentage of cells with 'active' nuclear STAT5 when the *Pkd1* gene is genetically altered, compared to wild-type control animals, suggesting that modulation of the *Pkd1* gene activates STAT5.

Figure 3: STAT5 in nuclear at 4, 8 and 10 week old Pkd1$^{nl/nl}$ mouse kidneys.

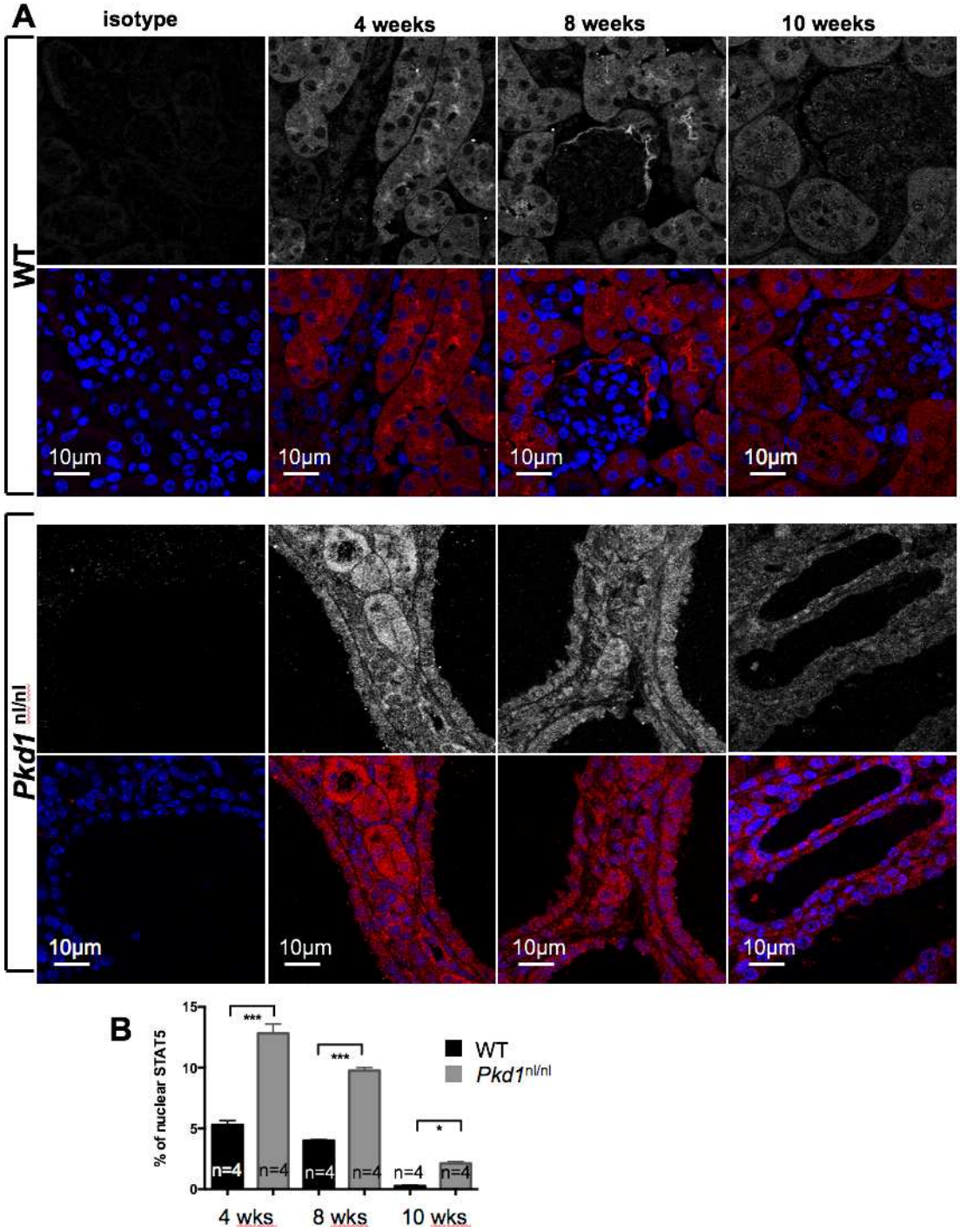

Because *Pkd1* is expressed in the liver and other tissues in addition to the kidneys, we next wished to inactivate *Pkd1* specifically in kidney epithelial cells and study whether this can also lead to STAT5 activation. To achieve this, we deleted *Pkd1* from renal epithelial cells using the kidney specific protein (ksp) promoter driving Cre-ERT2, previously published [18]. Thus Pkd1$^{fl/fl}$; Ksp-CreERT2 mice were given either a 3-day administration of tamoxifen to delete *Pkd1* (*Pkd1*$^{del/del}$) or vehicle control (*Pkd1*$^{fl/fl}$) and sacrificed at 11 and 16 weeks later. Analysis of multiple animals demonstrated that STAT5 was more strongly expressed in cyst lining cells of *Pkd1*$^{del/del}$ mice compared with the *Pkd1*$^{fl/fl}$ mice, which exhibited strong cytoplasmic STAT5 expression (compare Figure 4A with 4B). Quantification of nuclear, thus active, STAT5 expression indicated a statistically significant 2-fold increase in *Pkd1*$^{del/del}$ mice compared to *Pkd1*$^{fl/fl}$ mice, at both time points studied (Figure 4C, 11 weeks and 4D, 16 weeks). In addition, we performed Western blotting from kidney lysates of control or Pkd1$^{del/del}$ and found pYSTAT5 in Pkd1-null kidneys at 16 weeks with no evidence of phosphorylation in control animals (SI Fig1D). Collectively data from two independent ADPKD orthologous models show that deletion of *Pkd1* leads to increased nuclear STAT5, suggesting that *Pkd1* deletion acts as an activating signal for STAT5. We thus reasoned that STAT5 may represent a key player in ADPKD-pathogenesis by promoting enhanced proliferation.

Figure 4: STAT5 in KSP-cre driven deletion of *Pkd1*

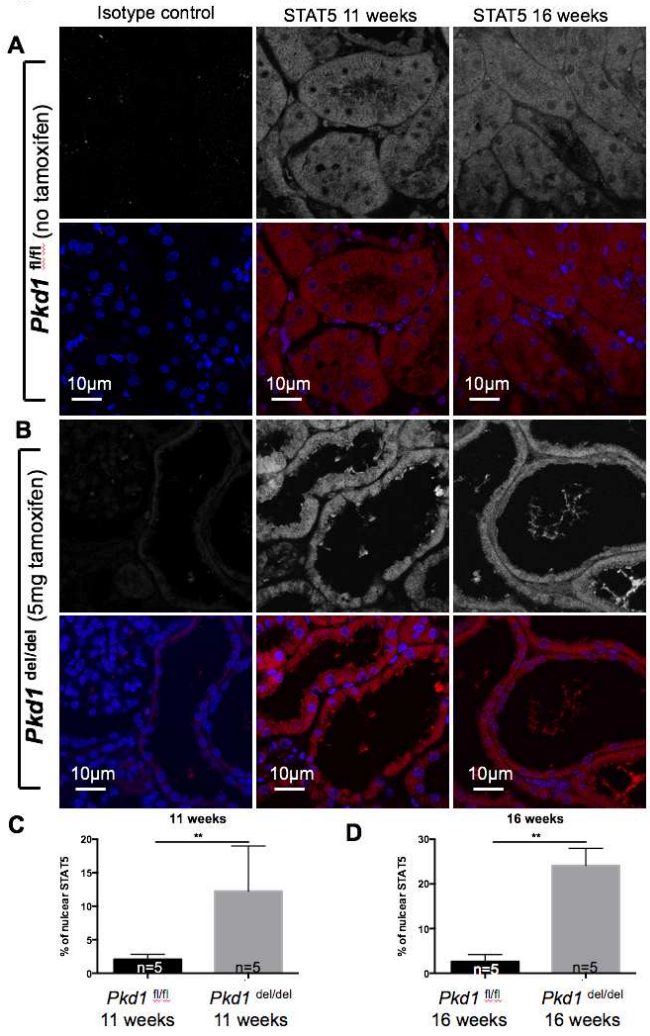

STAT5 antagonism reduces cyst growth *in vitro*

To study whether inhibition of the STAT5 pathway plays a role in cyst growth we grew OX161 or F1 mouse cells on basement membrane BD matrigel™. Cells formed several cysts within 24 hours which grew larger by 10 days-post-treatment (dpt) (Figure 5A). We found that the STAT5 inhibitor at day 1 post treatment (1dpt) and 10dpt did not significantly alter the cyst growth, however at 6dpt there was a significant decrease of the cyst growth compared to DMSO vehicle control (Figure 5B). We validated these results using an RNAi against STAT5. Similarly, to the pharmacological inhibitor treatment, siRNA mediated inhibition of STAT5 led to a significant reduction in cyst area when compared to non-target RNAi control transfected cells at both 6 and 10dpt (Figure 5C). To ensure that our results were not cell-type specific, we employed an additional 2 isogenic cell lines, with either intact Pkd1 (F1 mouse $Pkd1^{+/+}$) or cells that the Pkd1 gene was deleted (F1 mouse $Pkd1^{-/-}$). Inhibition of STAT5 led to a significant reduction in cyst growth in $Pkd1^{-/-}$ (Figure 5E) but had no effect in $Pkd1^{+/+}$ cells (Figure 5D). Taken together, these results corroborate that inhibition of STAT5 halts cyst growth *in vitro*.

Figure 5: STAT5 inhibition reduces cyst growth *in vitro*

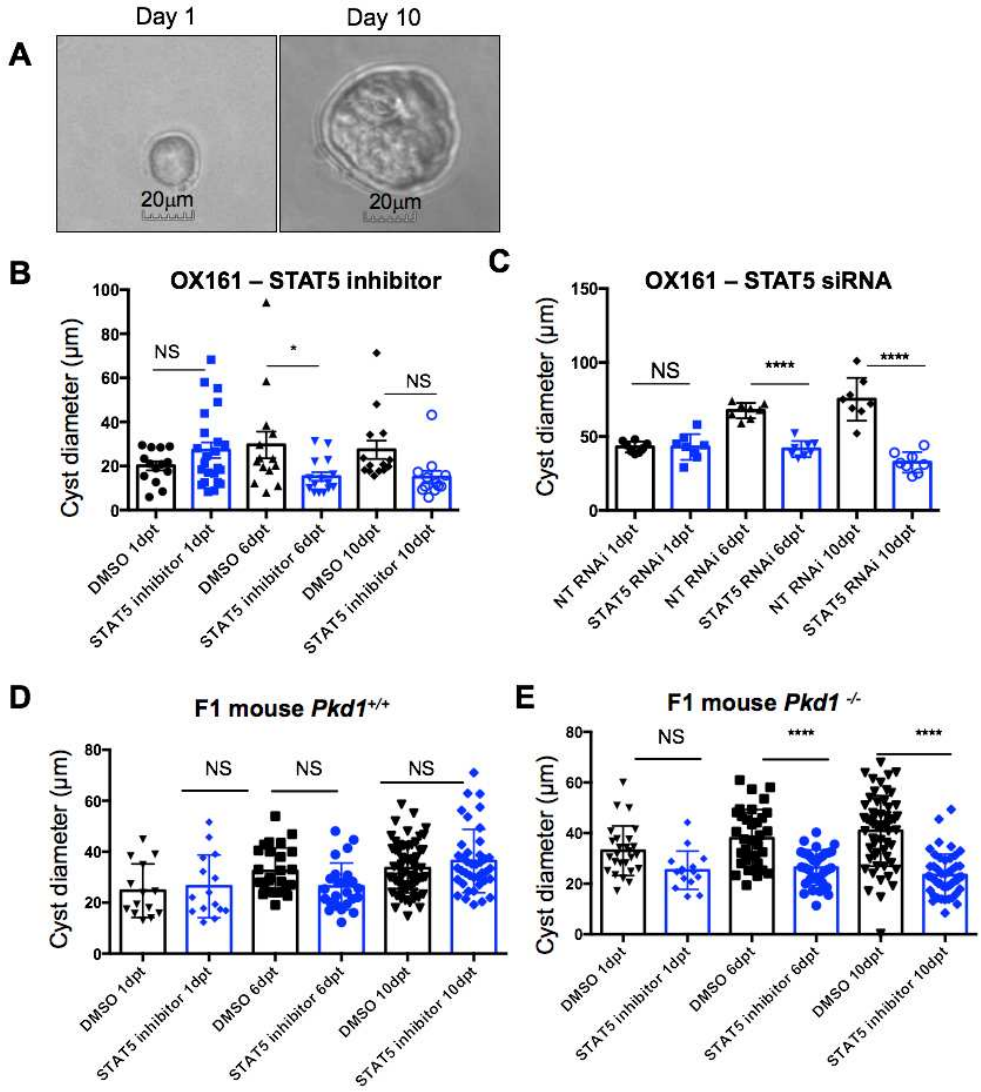

Overexpression of GH leads to high STAT5 activation and renal dilatation.

To test directly whether activation of STAT5, independently of the *Pkd1* status, in *Pkd1* wild-type mice, can drive enhanced kidney proliferation, we used transgenic mice that overexpress GH under the metallothionein promoter (GH^{tg}) [19, 20]. Firstly, we studied the morphology of the GH^{tg} and wild type kidneys by performing H&E staining. GH^{tg} mice were previously shown to exhibit polycystic kidneys [21]. We confirmed that the kidneys of GH^{tg} mice exhibited multiple renal tubular dilatations when compared to the kidneys of wild-type mice (Figure 6A). Immunohistochemistry using anti-STAT5 antibodies demonstrated that STAT5 was predominantly cytoplasmic in wild type animals but its expression was nuclear in GH^{tg} mice, suggesting that GH activated STAT5 in these kidneys (Figure 6B). Interestingly, nuclear STAT5 was found in dilated tubules (Figure 6B asterisk). To test whether 'activated' STAT5 correlates with an increase in proliferation we stained kidneys of wild type and GH^{tg} mice with cyclin D1, a well-known pro-proliferative gene shown here to promote cystic cell proliferation (Figure 1A). We observed higher cyclin D1 expression in GH^{tg} mice compared to wild type controls (Figure 6C). Rabbit IgG isotype control showed minimal background staining (Figure 6D). Collectively these data suggest that GH can drive aberrant activation of STAT5 in mouse kidney epithelial cells *in vivo*.

Next to test whether cyclin D1 was increased in the murine ADPKD models, and to study whether some cells were double positive for both cyclin D1 and STAT5, we stained serial kidney section from $Pkd1^{nl/nl}$ and $Pkd1^{del/del}$ mice with both STAT5 and cyclin D1. We found cyclin D1 expression was enhanced in cyst lining cells in both *Pkd1* models (SI Figures 2-3) and we consistently found STAT5-positive cyclin D1-positive double positive cells (arrows). These data indicate that cyclin D1 is abnormally activated in these cells.

Figure 6: GH enhances proliferation and activates STAT5 *in vivo*

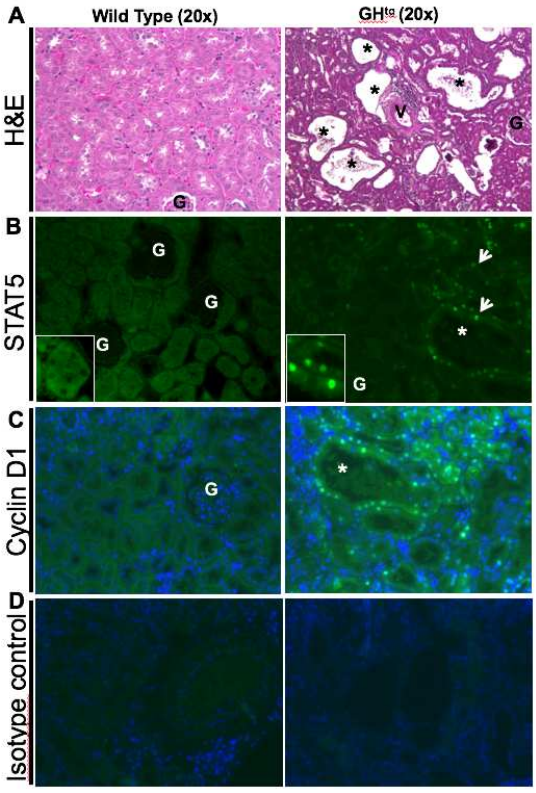

GH-induced proliferation is mediated via the STAT5-Cyclin D1 axis.

To investigate whether STAT5 can transcriptionally activate cyclin D1 in renal epithelial cells, we used transformed human derived *Pkd1 wild-type* tubular epithelial cells (UCL93) [15], where activation of STAT5 can be temporally controlled by exogenous recombinant GH. Stimulation of cells with GH led to a marked increase in nuclear STAT5 compared with vehicle-treated cells (Figure 7A). We performed chromatin immunoprecipitation (ChIP) experiments using anti-STAT5 antibodies to study the binding of STAT5 to the CCDN1 promoter. ChIPs revealed that stimulation with GH significantly increased association of STAT5 with the cyclin D1 promoter compared to vehicle-treated controls (Figure 7B). By contrast binding of histone H3 to the RPL30 gene (a positive control for the ChIP technique) was similar in vehicle- and GH-treated cells (Figure 7B). To test whether GH-induced proliferation can be reversed by silencing of cyclin D1, we use a specific siRNA against CCDN1 and found that silencing of cyclin D1 led to reduced proliferation (Figure7C). Collectively our data suggest that GH activated STAT5 enhances proliferation via cyclin D1 in normal renal epithelial cells; whether GH signalling is enhanced in human and murine models of ADPKD is currently unknown.

Figure 7: GH enhances proliferation in a STAT5 dependent manner.

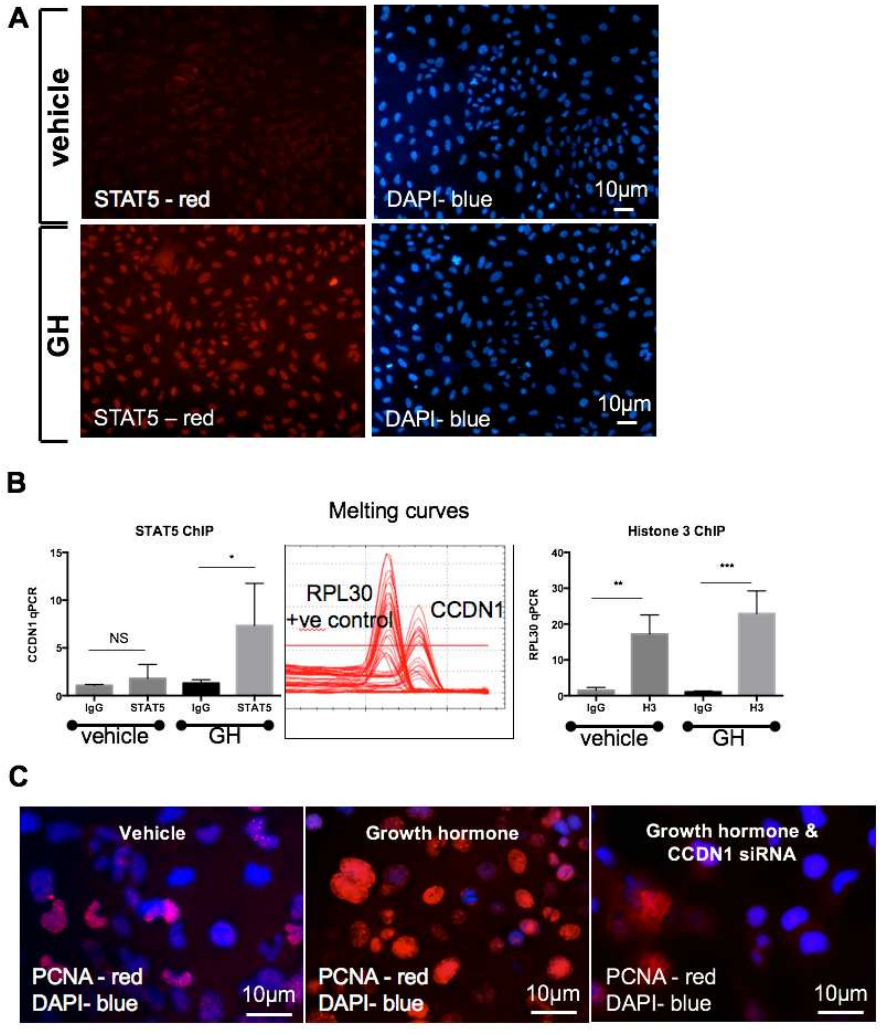

Serum GH is elevated in *Pkd1*$^{nl/nl}$ *mice.*

We next wished to study whether GH is abnormally expressed in murine ADPKD. Firstly, we investigated whether renal tubular epithelial cells express the GH-receptor (GHR), which is required to sense and respond to GH. To do this we stained sections of kidneys from multiple animals with an anti-GHR antibody and performed confocal microscopy. We found that both wild-type and Pkd1$^{nl/nl}$ animals express GHR in epithelial cells (Figure 8A). We also noted that GHR staining is punctate, consistent with 'activated' internalized receptor. GH is made by the pituitary gland and is found in serum, therefore, to study whether inactivation of *Pkd1* leads to elevated GH we collected serum from multiple animals at two different time-points, 5 and 10 weeks of age (representing early and late disease) from *Pkd1*$^{nl/nl}$ and corresponding wild-type controls. Flow-cytometry bead-based ELISAs were performed to measure levels of GH, and we found that Pkd1$^{nl/nl}$ animals have consistently higher circulating GH when compared to wild-type controls at both time-points studied (Figure 8B&C). Collectively, these data suggest that GH-initiated signalling is significantly more active in *Pkd1*$^{nl/nl}$ when compared to control, thus suggesting that GH may be underlying the atypical activation of STAT5 in murine ADPKD. Tissue-specific deletion of the GH gene is required to study the involvement of GH in driving ADPKD.

Figure 8: GH signalling in murine ADPKD

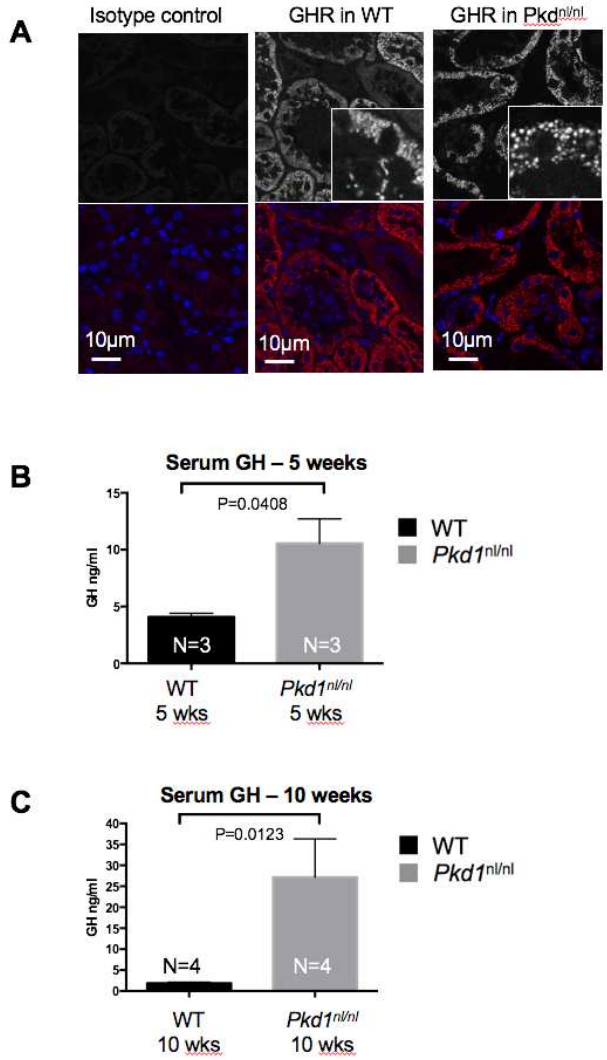

DISCUSSION

Mouse knockout studies have elucidated a clear role for STAT5 as a positive regulator of proliferation in epithelial non-renal tissues [22-24]; making STAT5 an attractive target to study in ADPKD. We report that STAT5 contributes to the pathogenesis of ADPKD by showing that (*i*) STAT5 is expressed in cyst-lining epithelial cells in two independent murine models of ADPKD, (*ii*) STAT5 controls proliferation of ADPKD-derived human epithelial cells (*iii*) inhibition of STAT5 results in reduced cyst growth *in vitro* (*iv*) GH activates STAT5 transcription leading to enhanced proliferation and (*v*) serum GH is elevated in the *Pkd1*$^{nl/nl}$ mouse. However, whether GH is elevated in human ADPKD remains unknown.

STAT5 knockout mouse studies have not reported any renal abnormalities making STAT5 a potential therapeutic target since it is not required for normal kidney function [22-24]. One strategy to inhibit STAT5 is via the use of JAK kinase inhibitors, which prevent STAT5 phosphorylation. The benefits of using JAK inhibitors include the subtype-selective inhibition of these enzymes and the fact that they are already approved to use in malignancies and rheumatoid arthritis [25-29]. To overcome toxicity, which can arise with some JAK inhibitors, a more targeted approach can be employed. For instance, targeting the SH2-domain of specific STATs could demonstrate selectivity with reduced side-effects. Here we used a selective small molecule STAT5 SH2-domain inhibitor that inhibits transcriptional output by blocking the interactions between STAT5 and SH2 domains, without affecting STAT3 or STAT1 [30]. Additional SH2 binders that selectively inhibit STAT5 at much lower concentrations have been generated [31]. Future animal studies are needed to compare the efficacy of the different STAT5 SH2 compounds in reducing cyst growth in ADPKD models. Alternatively, HDAC6 inhibition was recently shown to be effective in reducing cyst growth in murine PKD [32]; this is particularly relevant to this study because HDAC inhibition reduces STAT5 transcriptional activity [33], therefore use of selective HDAC inhibitors can be employed as an alternative strategy to inhibit atypical STAT5-initiated signalling.

Interestingly, STAT6, a known positive regulator of proliferation [34], is aberrantly activated in cyst-lining cells and its inhibition leads to reduced proliferation associated with a better outcome in murine ADPKD [10, 11]. In addition, a number of studies have demonstrated a pro-proliferative role for STAT3 in ADPKD (reviewed in [35]). Thus, we were surprised to find that neither STAT3 nor STAT6 silencing reduced proliferation of human ADPKD-derived epithelial cells; thus we conclude that our screen might underestimate the contribution of some JAK-STAT components. This could be explained by differences in the models used (murine ADPKD versus human ADPKD-derived cells). Alternatively, both STAT3/6 are known immune regulators and therefore may mediate their effects partly via acting on immune cells. Tissue-specific deletion of STATs is required in order to evaluate the contribution of the JAK-STAT pathway in molecular and genetic detail. Collectively, these findings highlight the complexity of the JAK-STAT pathway and the importance of using complementary cell culture and mouse models to study ADPKD.

Previously GH^{tg} mice were shown to exhibit a shorten life-span [36], chronic inflammation, increased cancer rates [37] and a profound cystic kidney phenotype already at a young age [21, 38]. Because GH is a potent activator of STAT5 [39-41] we used

GH^{tg} mice to study the effects of STAT5 activation in renal epithelial cells. Our work verifies the renal tubular dilatations, previously reported in GH-transgenic mice, and also demonstrates that STAT5 and Cyclin D1 are both activated in dilated tubules, suggesting that they contribute to tubular dilatation. Because GH^{tg} mice do not represent an ADPKD model, we then studied whether GH is elevated in an ADPKD mouse model. We show that circulating GH is elevated in serum of mice with ADPKD when compared to wild-type. This finding is important in relation to the ALADIN clinical trials; where use of the long-lasting somatostatin analogue octreotide, reduced mean total kidney volume at 1 year follow-up [42]. Interestingly, administration of octreotide has been shown to reduce circulating GH [43]. Thus, one alternative mechanism to explain the effects of octreotide is via inhibition of circulating GH and suppression of signalling triggered by STAT5.

Here we describe the first report of aberrantly-activated STAT5 expression in both human cystic cell lines and mouse models of ADPKD and show that mechanistically STAT5 drives proliferation partly via transcriptionally activating cyclin D1. The abnormal activation of STAT5 in ADPKD could be explained by a number of possible mechanisms, in addition to the effects of elevated serum GH. STAT3 and STAT6 become aberrantly activated by binding to a cleaved c-terminal fragment of *Pkd1* [35]. Therefore, potentially STAT5 activity may be enhanced via binding to *Pkd1*. However, tissue specific *Pkd1* knockout also leads to enhanced STAT5 activity, thus at least in mouse models, STAT5 does not physically interact with *Pkd1*. An alternative hypothesis is that inactivation of *Pkd1* genetically interacts with STAT5 via altering the balance of pro- and anti-proliferative signals. Indeed, *Pkd1* was shown to activate STAT1 transcription leading to an anti-proliferative and pro-quiescent phenotype in renal epithelial cells [9], this is consistent with the role of STAT1 as a strong anti-proliferative gene in cancer [44]. Thus, we hypothesize that in the absence of *Pkd1*, or when *Pkd1* expression is lowered, the anti-proliferative *Pkd1*-induced STAT1 pathway is inactivated (or its activity reduced) thus shifting the balance towards more proliferation via enhanced STAT5 activation.

In conclusion, we present the first data that identifies the growth-hormone-STAT5-Cyclin D1 axis as abnormally activated in ADPKD, leading to enhanced proliferation. Future studies are needed to selectively inhibit STAT5 in the kidney in order to test its putative pathogenic role in ADPKD.

METHODS

Animals. We used 40-day old iKSPCreER^{T2}/ *Pkd1*$^{fl/fl}$ mice, treated with tamoxifen (5mg) or vehicle for three consecutive days [18]. Mice were sacrificed at 11 or 16 weeks post-tamoxifen treatment. GH transgenics, where GH is driven by the metallothionein promoter were used [21]. *Pkd1*$^{nl/nl}$, harboring an intronic neomycin-selectable marker, or wild type littermate controls were used [45]. *Pkd1*$^{nl/nl}$ or control mice were sacrificed at 4-10 weeks of age and kidneys collected. Serum and kidney GH was measured using an ELISA (MPTMAG-49K, Millipore). All animal experiments were performed under the authority of a UK Home Office license.

Cell lines. Conditionally-immortalized *Pkd1* wild-type (UCL93) and ADPKD-derived lines (OX161 and SKI-001)[15] are tubular epithelial cells isolated from human kidneys and immortalized by transduction at an early passage (P1-4) with a retroviral vector containing a temperature-sensitive large T antigen and the catalytic subunit of human telomerase [46]. The F1-WT renal epithelial cells were previously isolated from kidney papillae of the Pkd1fl/fl mouse (B6.129S4-Pkd1tm2Ggg/J; the Jackson Laboratory). They were immortalized with the lentiviral vector VVPW/mTert expressing the mTert. To delete Pkd1 and produce F1/Pkd1-/- cells they were subsequently transfected with VIRHD/HY/Silntβ1/2363 lentivectors. Positive populations were selected by hydromycin selection [47]. Normal renal epithelial HKC-5 cells were previously isolated from a human nephrectomy specimen [48].

Protein biochemistry, ChIPs and antibodies. Cells were lysed using ice-cold Lysis Buffer (50mM Tris (pH 7.4) 250mM NaCl, 0.3% Triton X-100, 1mM EDTA) supplemented with protease inhibitor cocktail (Roche), freeze-thawed and sonicated. Whole cell lysates were boiled in 2xLaemmeli sample buffer for 5 minutes. Samples were resolved by SDS-PAGE and transferred using the Mini-PROTEAN system (Bio-Rad). Primary antibodies were anti-β-actin (ab8226, Abcam), anti-phosphorylated STAT5 (p-STAT5) (4322, Cell Signalling), anti-STAT5 (HPA027873, Sigma). Chromatin IPs were performed using SimpleChIP enzymatic chromatin IP kit with magnetic beads (9003, cell signalling), following manufacturer's instructions.

Immunofluorescence. Cells grown on coverslips were fixed in ice-cold methanol prior to blocking in 2% milk in TBST for 30 minutes and incubated with primary antibodies overnight at 4ºC. Antibodies used were: PCNA (2586, Cell Signalling (1:400), STAT5 (HPA027873, sigma (1:200)). Cells were washed and incubated with secondary anti-mouse AF488 (A-11001, Invitrogen (1:250) and anti-rabbit AF594 (A-11037, Invitrogen (1:250) antibodies. Microscopy was carried out using a confocal microscope. Quantification of fluorescence intensity was done by splitting the RGB image into individual channels, measuring mean grey value and calculating optical density using the formula OD=log (max intensity / mean intensity).

JAK-STAT inhibitors. VWR-573108 is a previously described STAT5 chromone-based inhibitor [16], also known as N'-(4-oxo-4H-chromen-3-yl)methylene) nicotinohydrazide was purchased from VWR (573108) and used at a final concentration of 100 μM. Cells were treated with equal volumes of DMSO as a vehicle control.

RNAi screen and transfections. 29 different RNAi smartpools from Dharmacon were used to reverse transfect the cystic cell line OX161 at a final concentration of 15 nM of RNAi using RNAiMAX reagent (Invitrogen) using manufacturer's

instructions. For individual line transfections, cells were reverse transfected with 20nM of Dharmacon gene specific RNAi using RNAi MAX transfection reagent (Invitrogen) following manufacturer's instructions.

Statistical analysis. All data were analysed with Prism Graphpad and Non-parametric, two-tailed, either Mann-Whitney T-tests or one-way ANOVA were performed and results with a P value of 0.05 or lower were considered significant.

Disclosure
None.

Acknowledgements
This work was supported by a Thomas-Berry and Simpson fellowship and a Kidney Research UK fellowship awarded to M Fragiadaki, Kidney Research UK project grant (RP40/2014, ACMO), grant SFB-F28 and SFB-F47 from the Austrian Science Fund (FWF; to B.M, M.T and R.M) and grant from the Dutch Technology Foundation Project 11823, (W.N.L.). The authors would like to thank the Sheffield RNAi screening facility, Ms Kimberley Veraar, Ms Josephine Pickworth and Ms Fiona Wright for technical support and Dr Roslyn J Simms for reading the manuscript and providing feedback.

FIGURE LEGENDS

Figure 1

JAK-STAT subset RNAi screen.

A. Cystic human tubular epithelial cells (OX161) were transfected in triplicate with one of the 29 RNAi sequences for 72 hours. Cells were then fixed and stained with PCNA and analysis of proliferation (PCNA) was performed by microscopy and scoring with Image J. **B.** Proliferation quantification of transcription factors, **C.** kinases, **D** receptors and **E** cytokines are shown. Silencing of core JAK-STAT components caused a significant change in proliferation of cystic tubular epithelial cells. Significant differences are shown with exact P values (** indicate P values of less than 0.0072 and * P values less than 0.05).

Figure 2

Proliferation is inhibited in cystic by inhibition of STAT5.

A. ADPKD-derived human epithelial cells, OX161 or SKI-001, were reversed transfected with either STAT5 or non-target siRNA and incubated for 72 hours (n=3). Cells were then fixed and stained with PCNA primary antibody and visualized using fluorescent microscopy using an anti-mouse cy3 secondary antibody (red), nuclei were counterstained with DAPI (blue). Analysis of data from three independent experiments is shown with P values indicated. **B.** STAT5 inhibitor (100μM) or DMSO were added to OX161 or SKI-001cells and 48 hours later cells were fixed and DAPI positive nuclei were counted to study cell numbers. Analysis of data from three independent experiments is shown with P values indicated. **C.** Flow cytometry for histone H3 (ser10) was carried out to determine whether silencing of STAT5 reduced mitosis when compared to non-target RNAi treated cells in two cell lines (OX161, left and SKI-001, right). **D.** OX161 cells were treated with 100μM of STAT5 inhibitor or equivalent volume of DMSO (1μL) for 48 hours. They were stained with cleaved caspase 3 (red) and nuclei were counterstained with DAPI (blue), representative pictures are shown. **D'.** Quantification of PCNA staining normalized for area of cells is shown. Analysis of data from three independent experiments is shown with P values indicated.

Figure 3

STAT5 expression in *Pkd1*$^{nl/nl}$ mice at 4, 8 and 10 weeks of age.

A. Representative images of kidneys sections stained with STAT5 (top panel, greyscale; lower panel, red) or isotype IgG control from 4 and 8 and 10-week old WT mice (top) and 4, 8 and 10-week old PKD1$^{nl/nl}$ mice (bottom). Nuclei were counterstained blue with TOPRO. Confocal microscopy was carried out at 63x magnification. **B.** Quantification of nuclear STAT5 in 4, 8 and 10 weeks old mice (n=4 mice in each group). Statistical analysis was performed using an unpaired one-way ANOVA.

Figure 4

STAT5 is nuclear in kidneys at both 11 and 16-week post deletion of murine *Pkd1*.

A. Predominantly cytoplasmic STAT5 staining was observed in Pkd1 intact control kidney tissues stained with a STAT5 antibody (top panel, greyscale; lower panel, red) and counterstained with TOPRO (blue) at both 11 and 16 weeks of age. Control isotype IgG staining was also performed. Representative pictures are shown. **B.** Nuclear STAT5 with some cytoplasmic staining was observed in ADPKD kidney sections stained with STAT5 antibody (top panel, greyscale; lower panel, red) in mice

with tamoxifen induced *Pkd1* inactivation at both 11 (n=5) and 16 weeks (n=5) of age. Control isotype IgG staining was also performed. Representative pictures are shown. **C.** Quantification of cells exhibiting nuclear STAT5 at 11 weeks and **D**. at 16 weeks is shown. To quantify image was split and threshold applied, using Image J, to count total number of nuclei then cells positive for nuclear STAT5 were counted manually, percentage of nuclear cells was calculated by dividing number of positive cells by total number of cells.

Figure 5
STAT5 inhibition reduces cyst growth *in vitro*.
A. Representative images of OX161, *PKD1* mutant cells, grown in BD-matrigel at day 1 (left panel) and day 10 (right panel). **B.** Inhibition of STAT5 with the use of 100μM of STAT5 inhibitor led to a significant reduction in cyst growth as measured at both 6-days post treatment (dpt), when compared to DMSO vehicle control; n=5. **C.** Inhibition of STAT5 using specific siRNAs also led to a significant reduction in cyst growth when compared to non-target RNAi control (NT RNAi), n=5. **D.** Inhibition of STAT5 with the use of the inhibitor at days 1, 6 and 10dpt in F1 Pkd1+/+ mouse cell line or **E.** the isogenic F1 Pkd1-/- line. One-way ANOVA test was used for statistical analysis.

Figure 6
GH enhances proliferation and activates STAT5 *in vivo*.
A. Representative pictures of hematoxylin and eosin staining are shown for WT kidneys (n=7) and GH^{tg} kidneys (n=8). G denotes the glomeruli, * indicates tubular dilatation and V, vessels. **B.** STAT5 immunohistochemistry was performed in both the WT and GH^{tg} mice and representative pictures are shown. Arrows point at strong STAT5 nuclear expression in dilated tubules. **C**. Immunohistochemistry for cyclin D1 was performed in WT and GH^{tg} mice and isotype control staining is shown in **D**.

Figure 7
GH enhances proliferation in a STAT5 dependent manner.
A. *PKD1* WT cells (UCL93) were treated with GH or vehicle control and stained with an anti-STAT5 antibody (red), nuclei were counterstained with DAPI (blue). Staining was analysed using a fluorescent microscope. **B.** ChIPs were performed for STAT5 or histone 3 (positive control, right panel) and quantitative PCR of the antibody associated chromatin was performed. Melting curves of the two primer sets (CCDN1 for STAT5 and PRL30 for histone H3) are shown in the middle panel. Data are expressed as fold enhancement over IgG. **C.** Cells were either transfected with a non-target RNAi or a CCDN1 specific siRNA and either treated with vehicle or GH, followed by staining with PCNA (red) and nuclei were counterstained with DAPI (blue).

Figure 8
Pkd1nl/nl exhibit elevated serum GH.
A. GHR staining in kidney section of WT mice (n=4) or mice with Pkd1 deletion, Pkd1nl/nl (n=4) was performed with anti-GHR antibodies and representative images are shown alongside isotype IgG contol. Anti-GHR is in greyscale/red, nuclei counterstain with TOPRO (blue), confocal images are shown at 63x magnification. **B & C**. Serum GH was measured in animals with intact Pkd1 (WT) or $Pkd1^{nl/nl}$ using a magnetic bead-based ELISA. Three animals per group were tested at 5 weeks of age

(B) and four animals per group at 10 weeks of age (C). ELISA results were subjected to student t-tests with any values lower than 0.05 considered significant.

Supplementary Figure 1.
A. Verification of silencing of STAT1, STAT3 and STAT5 was performed by Western blotting and amount of each protein was compared to that of non-target RNAi. β-actin acted as an internal loading control. **B.** Western blot was performed for pYSTAT5, total STAT5, pYSTAT3, total STAT3, pYSTAT1 and total STAT1 as well as β-actin which acted as a loading control. Human cells were treated either with IFN-α alone, to trigger JAK-STAT signalling, or IFN-α and STAT5 inhibitor simultaneously. These data illustrate that the STAT5 inhibitor blocks canonical pYSTAT5, without affecting total STAT5 and without affecting STAT1 and STAT3 phosphorylation. **C.** Flow cytometry was performed in Pkd1 WT and $Pkd1^{-/-}$ cells stained with an anti-P(ser10) histone H3 mitotic marker antibody, a representative flow chart for $Pkd1^{-/-}$ is shown. **C'.** Quantification of percentage of mitotic cells in both WT and F1 $Pkd1^{-/-}$ cells was carried out, there was no statistical difference in the WT cells but there was a statistically significant decline in % of mitotic cells in F1 $Pkd1^{-/-}$ cells. **D**. Western blot was performed using whole kidney lysates from WT and 11 or 16 weeks old mice after deletion of *Pkd1*. Blotting of membrane with phopshotyrosine STAT5 (pY STAT5) revealed a doublet, which corresponds to pYSTAT5a/b in *Pkd1* KO mice at 16 weeks of age. PCNA also revealed enhanced proliferation in *Pkd1* KO mice when compared to WT controls. β-actin was studied as an internal loading control.

Supplementary Figure 2.
A and B. Kidneys of $Pkd1^{nl/nl}$ mice at 6 (n=4) and 8 (n=4) weeks of age were stained with cyclin D1 (left panel) and STAT5 (right panel), and representative images of serial sections are shown with arrows pointing at cells exhibiting staining for both cyclin D1 and STAT5.

Supplementary Figure 3.
Serial section of the *Pkd1* KO mice at 11 weeks of age (n=5) were stained either with cyclin D1 (left) or STAT5 (right). Representative images are shown with arrows pointing to cells that express both cyclin D1 and STAT5.

REFERENCES

1. Ong AC, Devuyst O, Knebelmann B*, et al.* Autosomal dominant polycystic kidney disease: the changing face of clinical management. *Lancet* 2015; **385:** 1993-2002.

2. Qian F, Watnick TJ, Onuchic LF*, et al.* The molecular basis of focal cyst formation in human autosomal dominant polycystic kidney disease type I. *Cell* 1996; **87:** 979-987.

3. Grantham JJ, Chapman AB, Torres VE. Volume progression in autosomal dominant polycystic kidney disease: the major factor determining clinical outcomes. *Clinical journal of the American Society of Nephrology : CJASN* 2006; **1:** 148-157.

4. Foggensteiner L, Bevan AP, Thomas R*, et al.* Cellular and subcellular distribution of polycystin-2, the protein product of the PKD2 gene. *Journal of the American Society of Nephrology : JASN* 2000; **11:** 814-827.

5. Lanoix J, D'Agati V, Szabolcs M*, et al.* Dysregulation of cellular proliferation and apoptosis mediates human autosomal dominant polycystic kidney disease (ADPKD). *Oncogene* 1996; **13:** 1153-1160.

6. Torres VE, Higashihara E, Devuyst O*, et al.* Effect of Tolvaptan in Autosomal Dominant Polycystic Kidney Disease by CKD Stage: Results from the TEMPO 3:4 Trial. *Clinical journal of the American Society of Nephrology : CJASN* 2016.

7. Bjorklund M, Taipale M, Varjosalo M*, et al.* Identification of pathways regulating cell size and cell-cycle progression by RNAi. *Nature* 2006; **439:** 1009-1013.

8. Brooks AJ, Dai W, O'Mara ML*, et al.* Mechanism of activation of protein kinase JAK2 by the growth hormone receptor. *Science* 2014; **344:** 1249783.

9. Bhunia AK, Piontek K, Boletta A*, et al.* PKD1 induces p21(waf1) and regulation of the cell cycle via direct activation of the JAK-STAT signaling pathway in a process requiring PKD2. *Cell* 2002; **109:** 157-168.

10. Low SH, Vasanth S, Larson CH*, et al.* Polycystin-1, STAT6, and P100 function in a pathway that transduces ciliary mechanosensation and is activated in polycystic kidney disease. *Developmental cell* 2006; **10:** 57-69.

11. Olsan EE, Mukherjee S, Wulkersdorfer B*, et al.* Signal transducer and activator of transcription-6 (STAT6) inhibition suppresses renal cyst growth in polycystic kidney disease. *Proceedings of the National Academy of Sciences of the United States of America* 2011; **108:** 18067-18072.

12. Talbot JJ, Shillingford JM, Vasanth S*, et al.* Polycystin-1 regulates STAT activity by a dual mechanism. *Proceedings of the National Academy of Sciences of the United States of America* 2011; **108:** 7985-7990.

13. Leonhard WN, van der Wal A, Novalic Z*, et al.* Curcumin inhibits cystogenesis by simultaneous interference of multiple signaling pathways: in vivo evidence from a Pkd1-deletion model. *American journal of physiology Renal physiology* 2011; **300:** F1193-1202.

14. Takakura A, Nelson EA, Haque N*, et al.* Pyrimethamine inhibits adult polycystic kidney disease by modulating STAT signaling pathways. *Human molecular genetics* 2011; **20:** 4143-4154.

15. Parker E, Newby LJ, Sharpe CC*, et al.* Hyperproliferation of PKD1 cystic cells is induced by insulin-like growth factor-1 activation of the Ras/Raf signalling system. *Kidney international* 2007; **72:** 157-165.

16. Muller J, Sperl B, Reindl W*, et al.* Discovery of chromone-based inhibitors of the transcription factor STAT5. *Chembiochem : a European journal of chemical biology* 2008; **9:** 723-727.

17. Lantinga-van Leeuwen IS, Dauwerse JG, Baelde HJ*, et al.* Lowering of Pkd1 expression is sufficient to cause polycystic kidney disease. *Human molecular genetics* 2004; **13:** 3069-3077.

18. Lantinga-van Leeuwen IS, Leonhard WN, van der Wal A*, et al.* Kidney-specific inactivation of the Pkd1 gene induces rapid cyst formation in developing kidneys and a slow onset of disease in adult mice. *Human molecular genetics* 2007; **16:** 3188-3196.

19. Shaikh ZA, Smith JC. The biosynthesis of metallothionein rat liver and kidney after administration of cadmium. *Chemico-biological interactions* 1976; **15:** 327-336.

20. Blalock TL, Dunn MA, Cousins RJ. Metallothionein gene expression in rats: tissue-specific regulation by dietary copper and zinc. *The Journal of nutrition* 1988; **118:** 222-228.

21. Friedbichler K, Themanns M, Mueller KM*, et al.* Growth-hormone-induced signal transducer and activator of transcription 5 signaling causes gigantism, inflammation, and premature death but protects mice from aggressive liver cancer. *Hepatology* 2012; **55:** 941-952.

22. Cui Y, Riedlinger G, Miyoshi K*, et al.* Inactivation of Stat5 in mouse mammary epithelium during pregnancy reveals distinct functions in cell proliferation, survival, and differentiation. *Molecular and cellular biology* 2004; **24:** 8037-8047.

23. Nosaka T, Kawashima T, Misawa K*, et al.* STAT5 as a molecular regulator of proliferation, differentiation and apoptosis in hematopoietic cells. *The EMBO journal* 1999; **18:** 4754-4765.

24. Udy GB, Towers RP, Snell RG*, et al.* Requirement of STAT5b for sexual dimorphism of body growth rates and liver gene expression. *Proceedings of the National Academy of Sciences of the United States of America* 1997; **94:** 7239-7244.

25. Alimam S, McLornan D, Harrison C. The use of JAK inhibitors for low-risk myelofibrosis. *Expert Rev Hematol* 2015; **8:** 551-553.

26. Degryse S, Cools J. JAK kinase inhibitors for the treatment of acute lymphoblastic leukemia. *J Hematol Oncol* 2015; **8:** 91.

27. Harrison C. JAK inhibitors and myelofibrosis, Einstein and ruxolitinib. *Haematologica* 2015; **100:** 409-411.

28. Tanaka Y. Recent progress and perspective in JAK inhibitors for rheumatoid arthritis: from bench to bedside. *J Biochem* 2015; **158:** 173-179.

29. Verstovsek S. Therapeutic potential of JAK2 inhibitors. *Hematology / the Education Program of the American Society of Hematology American Society of Hematology Education Program* 2009**:** 636-642.

30. Li WX. Canonical and non-canonical JAK-STAT signaling. *Trends Cell Biol* 2008; **18:** 545-551.

31. Page BD, Khoury H, Laister RC*, et al.* Small molecule STAT5-SH2 domain inhibitors exhibit potent antileukemia activity. *Journal of medicinal chemistry* 2012; **55:** 1047-1055.

32. Cebotaru L, Liu Q, Yanda MK*, et al.* Inhibition of histone deacetylase 6 activity reduces cyst growth in polycystic kidney disease. *Kidney international* 2016; **90:** 90-99.

33. Pinz S, Unser S, Buob D*, et al.* Deacetylase inhibitors repress STAT5-mediated transcription by interfering with bromodomain and extra-terminal (BET) protein function. *Nucleic Acids Res* 2015; **43:** 3524-3545.

34. Wurster AL, Withers DJ, Uchida T*, et al.* Stat6 and IRS-2 cooperate in interleukin 4 (IL-4)-induced proliferation and differentiation but are dispensable for IL-4-dependent rescue from apoptosis. *Molecular and cellular biology* 2002; **22:** 117-126.

35. Weimbs T, Talbot JJ. STAT3 Signaling in Polycystic Kidney Disease. *Drug Discov Today Dis Mech* 2013; **10:** e113-e118.

36. Bartke A, Chandrashekar V, Bailey B*, et al.* Consequences of growth hormone (GH) overexpression and GH resistance. *Neuropeptides* 2002; **36:** 201-208.

37. Orian JM, Tamakoshi K, Mackay IR*, et al.* New murine model for hepatocellular carcinoma: transgenic mice expressing metallothionein-ovine growth hormone fusion gene. *J Natl Cancer Inst* 1990; **82:** 393-398.

38. Wanke R, Hermanns W, Folger S*, et al.* Accelerated growth and visceral lesions in transgenic mice expressing foreign genes of the growth hormone family: an overview. *Pediatr Nephrol* 1991; **5:** 513-521.

39. Manabe N, Kubota Y, Kitanaka A*, et al.* Src transduces signaling via growth hormone (GH)-activated GH receptor (GHR) tyrosine-phosphorylating GHR and STAT5 in human leukemia cells. *Leuk Res* 2006; **30:** 1391-1398.

40. Tiulpakov A, Rubtsov P, Dedov I*, et al.* A novel C-terminal growth hormone receptor (GHR) mutation results in impaired GHR-STAT5 but normal STAT-3 signaling. *J Clin Endocrinol Metab* 2005; **90:** 542-547.

41. Wang X, Darus CJ, Xu BC*, et al.* Identification of growth hormone receptor (GHR) tyrosine residues required for GHR phosphorylation and JAK2 and STAT5 activation. *Mol Endocrinol* 1996; **10:** 1249-1260.

42. Caroli A, Perico N, Perna A*, et al.* Effect of longacting somatostatin analogue on kidney and cyst growth in autosomal dominant polycystic kidney disease (ALADIN): a randomised, placebo-controlled, multicentre trial. *Lancet* 2013; **382:** 1485-1495.

43. Masuda A, Shibasaki T, Kim YS*, et al.* The somatostatin analog octreotide inhibits the secretion of growth hormone (GH)-releasing hormone, thyrotropin, and GH in man. *J Clin Endocrinol Metab* 1989; **69:** 906-909.

44. Johnson MR, Valentine C, Basilico C*, et al.* FGF signaling activates STAT1 and p21 and inhibits the estrogen response and proliferation of MCF-7 cells. *Oncogene* 1998; **16:** 2647-2656.

45. Happe H, van der Wal AM, Salvatori DC*, et al.* Cyst expansion and regression in a mouse model of polycystic kidney disease. *Kidney international* 2013; **83:** 1099-1108.

46. O'Hare MJ, Bond J, Clarke C*, et al.* Conditional immortalization of freshly isolated human mammary fibroblasts and endothelial cells. *Proceedings of the National Academy of Sciences of the United States of America* 2001; **98:** 646-651.

47. Lee K, Boctor S, Barisoni LM*, et al.* Inactivation of integrin-beta1 prevents the development of polycystic kidney disease after the loss of polycystin-1. *Journal of the American Society of Nephrology : JASN* 2015; **26:** 888-895.

48. Racusen LC, Monteil C, Sgrignoli A*, et al.* Cell lines with extended in vitro growth potential from human renal proximal tubule: characterization, response to inducers, and comparison with established cell lines. *J Lab Clin Med* 1997; **129:** 318-329.